



High-performance, additively-manufactured atomic spectroscopy apparatus for portable quantum technologies

S. H. MADKHALY,^{1,2}  N. COOPER,^{1,4} L. COLES,³ AND L. HACKERMÜLLER^{1,5}

¹*School of Physics and Astronomy, University of Nottingham, University Park, Nottingham NG7 2RD, UK*

²*Department of Physics, Jazan University, Jazan, Saudi Arabia*

³*Added Scientific Ltd, Unit 4, Isaac Newton Centre, Nottingham NG7 2RH, UK*

⁴*nathan.cooper@nottingham.ac.uk*

⁵*lucia.hackermuller@nottingham.ac.uk*

Abstract: We demonstrate a miniaturised and highly robust system for performing Doppler-free spectroscopy on thermal atomic vapour for three frequencies as required for cold atom-based quantum technologies. The application of additive manufacturing techniques, together with efficient use of optical components, produce a compact, stable optical system, with a volume of 0.089 L and a weight of 120 g. The device occupies less than a tenth of the volume of, and is considerably lower cost than, conventional spectroscopic systems, but also offers excellent stability against environmental disturbances. We characterise the response of the system to changes in environmental temperature between 7 and 35 °C and exposure to vibrations between 0 - 2000 Hz, finding that the system can reliably perform spectroscopic measurements despite substantial vibrational noise and temperature changes. Our results show that 3D-printed optical systems are an excellent solution for portable quantum technologies.

Published by Optica Publishing Group under the terms of the [Creative Commons Attribution 4.0 License](https://creativecommons.org/licenses/by/4.0/). Further distribution of this work must maintain attribution to the author(s) and the published article's title, journal citation, and DOI.

1. Introduction

Experiments involving cold atoms allow high-precision tests of fundamental physics [1–6], simulation of condensed matter systems [7–9] and the study of new states of matter [10–13]. They also offer one of the most promising routes towards quantum information processing [14–16] and quantum communication [17–20]. Furthermore, the techniques used in these experiments underpin an important emerging field of technological development, in the form of atomic quantum sensors and cold atom clocks [21–24].

These experiments require one or more lasers to be frequency-stabilised via feedback based on thermal vapour spectroscopy, and most require the production of a magneto-optical trap (MOT) [25]. The frequency stability of these lasers is key to the performance of the experiment, yet the optical systems used for vapour spectroscopy are often not well-optimised, bulky and occupy a large fraction of an optical table. Recently, the use of additive manufacturing (AM, also known as 3D printing) methods, together with novel approaches to experimental design, has been demonstrated to enable a compact magneto-optical trap system that captures $> 2 \times 10^8$ atoms [26,27]. AM techniques allow devices to be fully optimised for their intended function, without reference to traditional design constraints [28].

Herein, we apply these broader principles to the construction of a separate, specialised device for laser frequency stabilisation and characterise its performance under environmental stress such as temperature changes and vibrations. While the specific prototype device we demonstrate as an example is aimed at applications within atomic physics, the techniques and design principles

employed are transferable and may be of use in any field relying on hitherto complex free-space optics.

Our methods have been deliberately chosen so as to facilitate replication and augmentation of this approach: we focus on low-cost, widely-available hardware components and open source software, while keeping the complexity of the techniques and devices employed to a minimum. Our AM-based approach enables remarkable stability and robustness against environmental changes and makes devices constructed along these lines a cost-effective option for deployment in quantum technologies. For portable quantum technologies [29–31] and fundamental experiments in space [32–35], stability with respect to temperature changes and vibrations is of key importance. The device demonstrated here also employs an unconventional spectroscopy scheme, in which light resonant with two different atomic transitions is spatially-overlapped in the atomic vapour, that has been found to offer some advantages in terms of signal strength and sensitivity [36]. The different features and components of the device are discussed in more detail below.

2. Monolithic optomechanical framework

Our prototype device consists of a monolithic, AM framework that is populated with off-the-shelf optical components, as seen in Fig. 1.

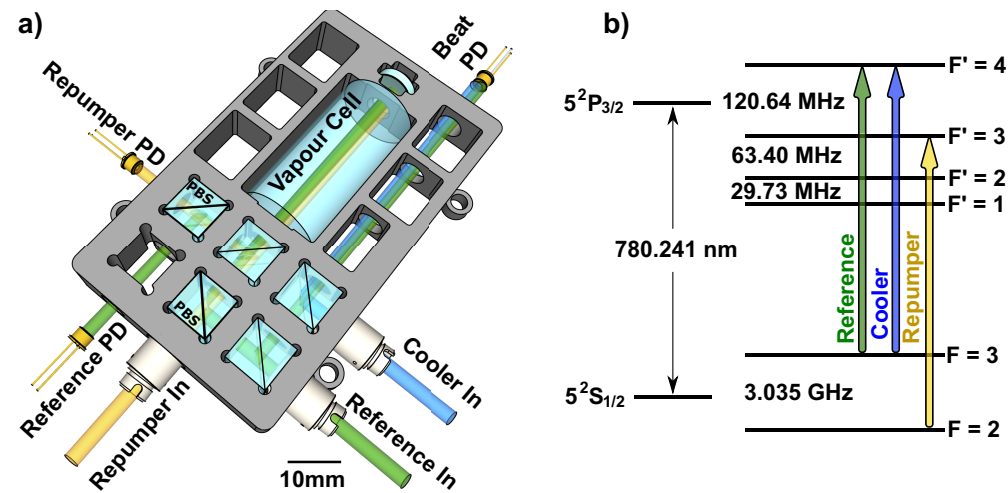


Fig. 1. a) Compact system for performing spectroscopic measurements on three lasers simultaneously, exploiting a monolithic, additively manufactured frame. b) Transition structure of the ^{85}Rb D2 line, indicating the names traditionally given to lasers used for magneto-optical trapping and cold atom experiments, as well as the transitions they address.

This framework was additively manufactured from polylactic acid via Fused Deposition Modelling (FDM) printing [37–39] and designed to house a minimal optical setup for simultaneous frequency stabilisation of three lasers via saturated absorption spectroscopy [40]. The total print time was about 3 hours with no post processing required. A model of the framework, with optical components implanted, is shown in Fig. 1, and the relevant beam pathways are shown schematically in Fig. 2.

The device has outer dimensions of $110 \times 65 \times 12.5$ mm and a total weight of 120 g (including optics). The design of the framework keeps optical path lengths as short as possible to improve stability. The maximum optical path length for any of the beams in the device is 230 mm, while a typical path length in a standard experimental apparatus would be on the order of 1–2 m. Stability is also achieved by omitting adjustable elements.

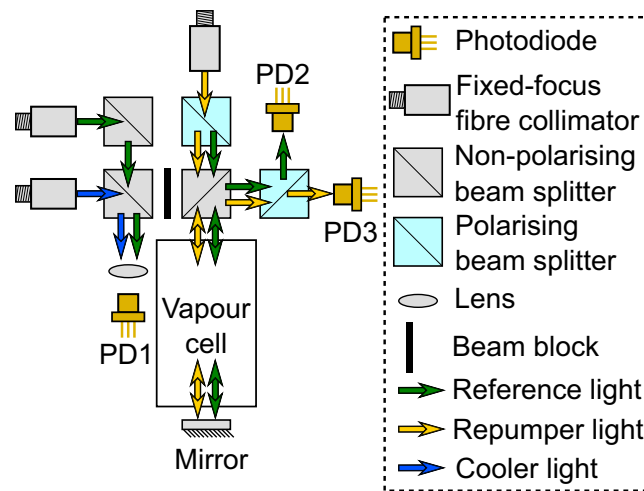


Fig. 2. Schematic diagram showing the optical pathways within the compact spectroscopy device.

The optical components push-fit directly into the polymer framework, exploiting AM design features described in more detail in [27]; holes in the framework allow the passage of the laser beams where required and recesses over the central regions of the optics allow them to be slotted into the framework without risk of scuffing the optically-active surfaces. Small holes in the corners of the component slots improve push-fit alignment by favouring an extended contact region rather than a point contact, and also avoid the build defects that can otherwise result from filament dragging [41]. A grid-like structure adds stability, reduces material and supports a homogeneous printing process. The layout of the beam paths is shown in Fig. 2.

3. Optical components and pathways, control electronics

The layout of the spectroscopy apparatus is shown in Fig. 1 (a). All components are of industry standard sizes and the device can be reproduced with components from a range of manufacturers. Fig. 2 shows the schematic outline of the optical pathways within the device, indicating how light from each of the three input connectors is employed to generate the required spectroscopic signals and optical beat note. The photodiodes are operated using homebuilt transimpedance amplifiers with buffered outputs. The LM324N quadruple operational amplifier chip is employed for the spectroscopic photodiodes and the (higher bandwidth) AD8001A operational amplifier is used for the optical beat note (note that some data was collected using commercial photodiode-amplifier packages, prior to the construction of the homebuilt models — see e.g. Fig. 6).

All beams are brought into the optical framework via fixed-focus fibre collimators and then distributed and routed via beam splitters. Fig. 2 shows a diagram of the beam paths. The reference beam is immediately split into two pathways: one for vapour spectroscopy and one to produce an optical beat note. The component used for the optical beat note is combined with the cooler light, at a non-polarising beam splitter, following which the two beams are overlapped on the photodiode ‘PD1.’ The component to be used for spectroscopy is combined at a polarising beam splitter with the repumper light. The two beams then propagate through the vapour cell and back, with a portion of the return light picked-off using a non-polarising beam splitter; the reference and repumper frequency components of the return light are then separated via a polarising beam splitter and directed onto photodiodes ‘PD2’ and ‘PD3’ respectively. The double-pass beam configuration within the vapour cell [36] allows for Doppler-free spectroscopy to be performed,

resulting in the saturated absorption signal of D2 line of ^{85}Rb and ^{87}Rb shown in Fig. 3 (a). The device also produces an optical beat note (Fig. 3 (b)), on photodiode PD1, which allows the cooler laser to be stabilised with a controllable frequency separation from the reference laser.

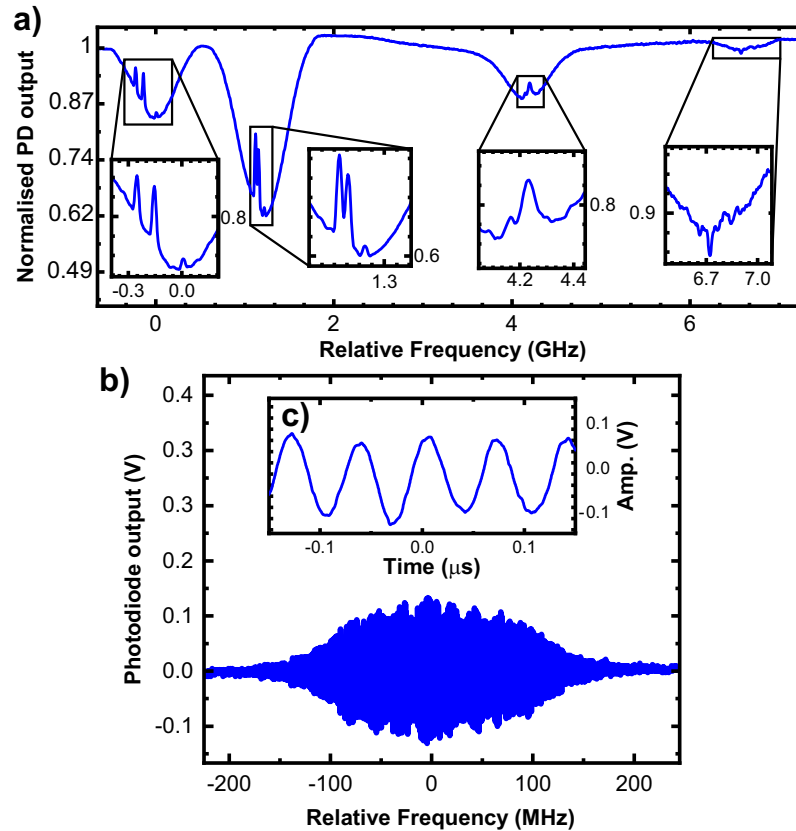


Fig. 3. Saturated absorption spectra of ^{85}Rb and ^{87}Rb isotopes (a), and beat signal between a laser tuned to the ^{85}Rb cooler transition and the reference laser (b), both obtained using the optical system illustrated in Fig. 1. The inset (c) displays a single-frequency beat note at (13.4 ± 0.1) MHz.

Fig. 3 (b) shows the beat note created between the reference laser and the cooler laser, obtained from the reference laser being stabilised to the ^{85}Rb $F = 3 \rightarrow F' = 4$ transition and the cooler laser being scanned over the full range. The main panel shows the beat signal envelope as the cooler laser is scanned; this gives an indication of the frequency range and signal to noise ratio of the beat signal, but necessarily undersamples the individual beat frequencies present at any given point within the scan; the inset therefore displays an example of a single-frequency beat note at (13.4 ± 0.1) MHz.

To improve the laser frequency stability while reducing size, weight and cost, control electronics based on digital microcontrollers were utilised. Specifically, the Arduino Uno development board was used, in combination with its associated open-source software, as the central component of our control and feedback electronics.

The system has been tested using both external cavity diode lasers (e.g. for the data in Fig. 7) and distributed feedback lasers (e.g. as used for Figs. 3(a) and 4). A $1/e^2$ beam diameter of 2.1 mm was used and spectroscopy signals were obtained with beam powers ranging from 0.5 to 5 mW. By dividing the r.m.s. voltage noise on the gradient of the spectroscopic signal (which is

typically used as a feedback signal for laser frequency stabilisation) by its sensitivity to frequency variations about the laser lock point, we estimate the spectroscopic limit on laser linewidth using our current system, with a feedback bandwidth of 10 kHz, to be (1.28 ± 0.02) MHz. This would be more than sufficient for most applications, such as the creation of a magneto-optical trap (shown in [27]), though certain specialist applications may require narrower linewidths. These could be obtained at relatively modest cost through the use of superior photodiode amplifiers; alternatively, if the majority of the contributions to the free-running laser's frequency variations come from the low-frequency end of the spectrum, as is usually the case, then the spectroscopic output can be time-averaged or put through a low-pass filter to improve signal-to-noise by sacrificing bandwidth.

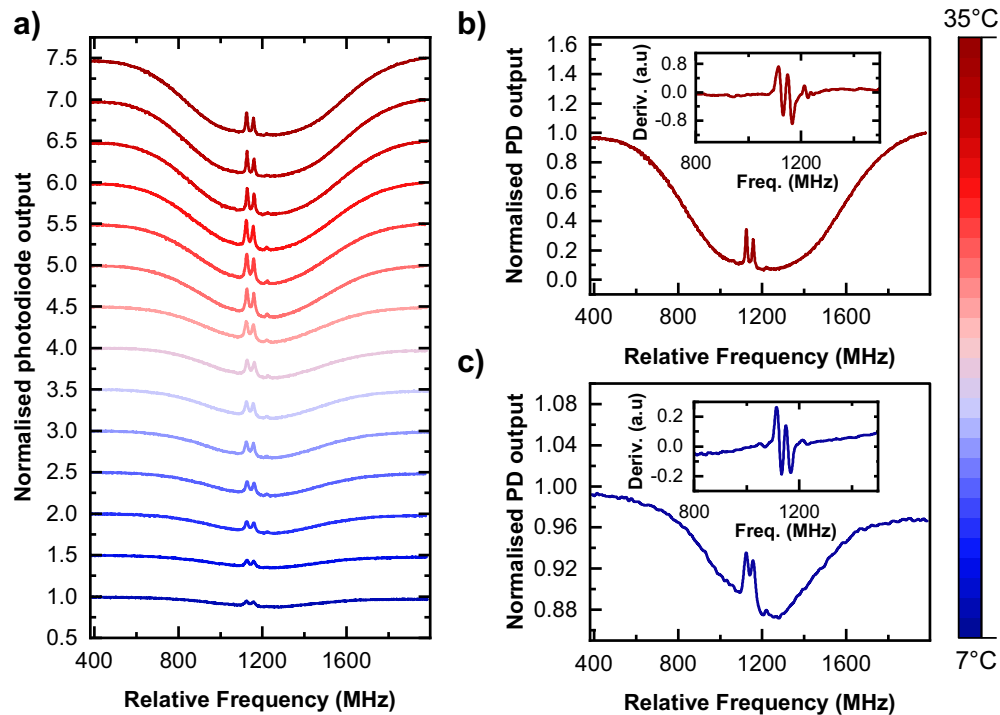


Fig. 4. (a) Spectroscopic signal line shape of ^{85}Rb $F = 3 \rightarrow F' = 2, 3, 4$ transition corresponding to temperature changes from 7°C to 35°C . For visibility, an offset of 0.5 is applied between successive traces. As the temperature rises from 7°C (panel (c)) to 35°C (panel (b)), the spectroscopic signal amplitude increases while its form remains unchanged. The insets in (b) and (c) represent the derivative signals of the corresponding traces.

4. Stability measurements

To ensure that our system is suitable for use outside the laboratory, a series of stability tests under harsh environmental conditions was performed.

4.1. Thermal stability test

In order to test the optical system's thermal stability, it was subjected to changes in the environmental temperature while monitoring the resulting spectroscopic signals. The optical framework was placed inside an aluminium box to create a uniform thermal distribution around the system, and the temperature was gradually raised using a heating tape. This process was

performed sufficiently slowly to ensure that the system reached thermal equilibrium prior to data collection. The change in temperature was monitored using three temperature and humidity sensors placed at different points inside and outside the metal box. The laser frequency was continuously scanned across the $F = 3 \rightarrow F' = 2, 3, 4$ transitions of the ^{85}Rb D2 line, in order to measure the system's response to the temperature changes. The spectroscopic signal was captured at a range of temperatures and is plotted in Fig. 4.

As seen in the figure, the device performs its intended function over the full temperature range, from 7°C to 35°C . The form of the spectroscopic response is largely unchanged, while its amplitude increases at higher temperatures due to the increased vapour pressure of the alkali metal within the vapour cell. The spectroscopy traces for the highest (35°C) and lowest temperatures (7°C) are shown separately in Fig. 4 (b), (c). The derivatives for these traces are given in the insets and depict an error signal with good signal-to-noise. The observed performance is at least comparable to that reported for considerably more expensive systems, made out of materials specifically selected for thermal stability, such as Invar and Zerodur [42].

The derivatives according to frequency have been calculated for all traces shown in Fig. 4 (a), together with additional data of the same nature that was omitted from Fig. 4 (a) to avoid overcrowding, and were used to obtain a quantitative, temperature dependent comparison of the relative capture range and the relative stabilisation signal gradient. Figure 5 shows the variation of the sensitivity of a laser stabilisation feedback signal (corresponding to the gradient of the spectroscopic signal) to laser frequency (blue data points), normalized to the result at lab temperature (20°C). In order to obtain these results, the first and second derivatives of the spectroscopic signals were obtained via a 3-point central difference method. Since the dominant source of error in the plotted data comes from high-frequency electrical noise in the photodiode amplifier circuit, such that the noise contributions even to adjacent sample points show very little correlation, multiple gradient estimates with different sample widths can be used to obtain an average value and associated statistical error estimate, which is plotted in the figure.

The dash-dotted green line indicates the expected variation due to vapor pressure changes; we obtain this result by assuming that all points in the observed signal individually obey the Beer-Lambert law, and that the absorption coefficient for each laser frequency scales in proportion to the vapor pressure in the cell. This model is sufficient to yield most of the variation observed over the relevant parameter range. It can be seen that our experimental data shows a slightly stronger temperature response, particularly in the higher temperature range. This can be attributed to the fact that our model neglects saturation effects; at high vapor pressure, the increased attenuation of the light reduces the saturation level, and consequent power broadening, that occurs at positions further along the optical path. This reduction in power broadening sharpens the sub-Doppler features slightly and hence can be expected to lead to a small increase in the gradient of the stabilisation signal, as observed. Importantly, our results do not indicate any degradation of the performance of the spectroscopic system over the full temperature window.

Also plotted is the relative capture range of the stabilisation signal (orange data points); this is given by the frequency range about the desired stabilisation frequency within which the gradient of the feedback signal does not change sign, normalised to the result at lab temperature (20°C). This parameter is a measure of the robustness of a laser stabilisation technique. Derivative and error determination relies on a 3-point central difference approach, together with standard error propagation to convert uncertainty in the values of the second derivative of the spectroscopic signal to uncertainty in the laser frequency at which it changes sign. The results show that the performance of the spectroscopic system is not degraded as the temperature moves away from the standard operating temperature of 20°C . The slight downward trend in capture range as temperature is increased can be attributed to the same mechanism of reduced power-broadening as described above.

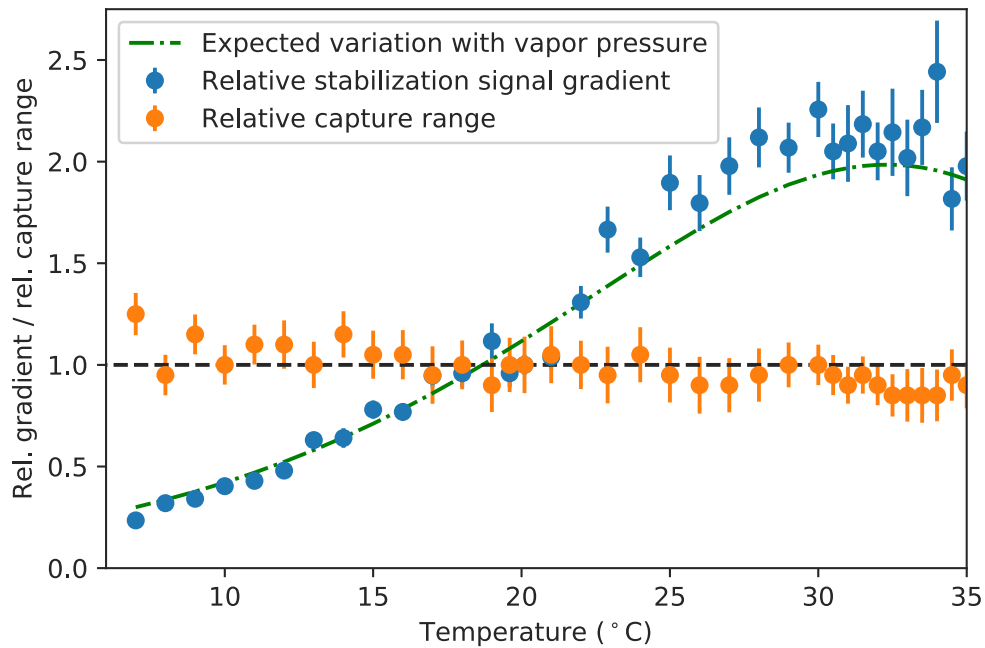


Fig. 5. Relative sensitivity of laser stabilisation feedback signal (given by the maximum second derivative of the spectroscopic signal with respect to laser frequency) as a function of device temperature (blue data). The green line indicates the expected variation due to the change in Rb vapor pressure. The orange data shows the capture range. In both cases, normalization is relative to the values measured at 20 °C.

4.2. Response to vibrations

Mechanical instability is a major challenge that needs to be overcome when designing portable systems for space applications and work outside laboratory walls [43]. For this purpose, we simulated a vibrating environment by placing the device onto an aluminium plate, as shown in Fig. 6.

An analog monitoring accelerometer (Te-connectivity 820M1), placed as shown in the figure, was used to measure and record the vibrations to which the device was exposed. Sinusoidal vibrations were introduced at several frequencies, between 0 Hz and 2 kHz, generated by a frequency generator and a loudspeaker. Additionally, manual shaking of the plate was used to simulate a noisy environment.

Figure 7 displays the power spectral density of the control voltage used to drive the loudspeaker (black, lowest panel), the measured acceleration of the vibrating plate (orange), and the resulting photodiode output voltages from the reference photodiode, PD2, with the laser's frequency stabilisation active (green) and inactive (blue). For reference, the DC voltage level of the photodiode output voltages was ~ 50 mV. This is shown for driving frequencies of 100 Hz, 500 Hz, 1 kHz and 2 kHz (panels a) to d) respectively) as well as for manual shaking (panel e)). For sinusoidal, single-frequency vibrations, an amplitude of ± 0.2 ms⁻² was applied, corresponding to the maximum output of the speaker. For the random shaking test (panel e)), vibrations were applied both manually and through the loudspeaker, with amplitudes going far beyond what was possible with the speaker alone; corresponding data was collected at frequencies up to 15 kHz. Despite clear contributions to the measured acceleration spectrum, very little contribution is made to the power spectrum of the optical signal by the presence of vibrations.

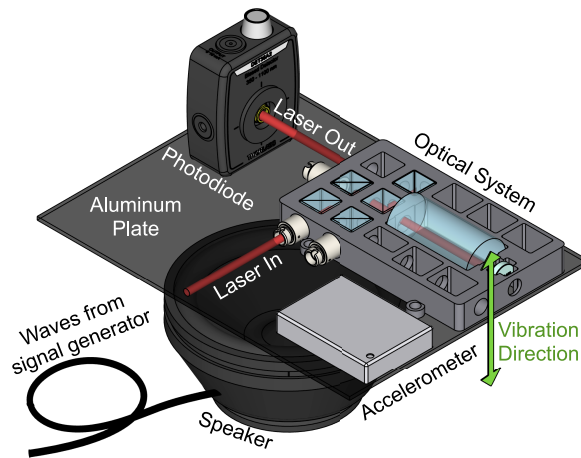


Fig. 6. Mechanical stability test setup. A loudspeaker was used to generate a vibrating environment with varying frequencies to evaluate the optical framework's stability — see text for details.

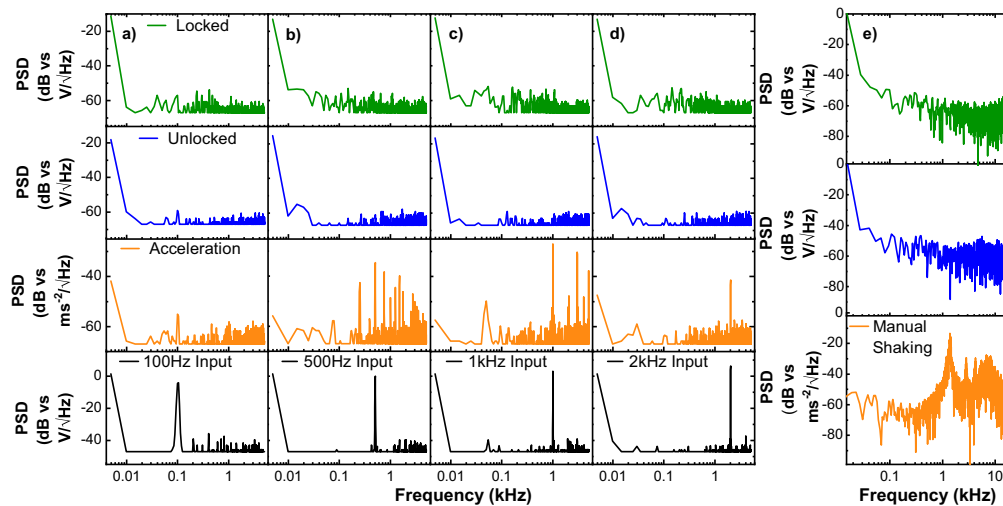


Fig. 7. Measurements of the optical system's response to single-frequency vibrations (100Hz, 500Hz, 1kHz, 2kHz) generated from a loudspeaker (a,b, c, and d) and to manual shaking (e). The power spectral density (PSD) of the output signal from the reference photodiode (PD2) is shown as a function of frequency, both when the laser is stabilised on resonance with the $^{85}\text{Rb } F = 3 \rightarrow F' = 4$ transition (green), and when the laser is free-running about the same frequency (blue). The PSD of the vibrations measured by 820M1-TE accelerometer (see Fig. 6) is also shown (orange), along with the PSD of the driving voltage applied to the loudspeaker (black).

A requirement for a device to be suitable for portable quantum technologies is that it can withstand the acceleration and vibrations caused by transportation, e.g. those experienced in a moving vehicle [44] or during a space launch [45], then operate in a stationary but un-isolated environment. Our data shows that the device described herein can operate well not only after, but also during, manual shaking, which produced acceleration amplitudes comparable to those experienced during high-speed transportation [44,45]. Perturbation in an uncontrolled but stable environment outside the lab (e.g. standing on the ground or on a platform) are likely to be of similar amplitudes to what we have tested in Fig. 7.

The advantages of the 3D printed setup can be qualitatively illustrated by comparison to a conventional system. For these measurements, the aluminium plate shown in Fig. 6 was cantilevered from the side of a standard optical bench. Data was simultaneously collected from both the compact spectroscopy apparatus on the vibrating plate and from a conventional spectroscopy apparatus located approximately two meters away on the optical bench. This apparatus employed a 130 cm optical beam pathway from an external cavity diode laser (inside a Toptica TA pro box), through a total of six mirrors on standard kinematic mounts, terminating on a Thorlabs PD10A amplified photodiode. Note that the light was sourced from the same laser for both measurements, so disturbance of the laser cannot explain the observed differences. Fig. 8 shows a comparison of the performance of the two systems. Fig. 8(a) shows that the form of the Doppler-free spectroscopy signal obtained from our compact spectroscopy device, mounted directly onto the vibrating plate, was barely affected by the presence of the vibrations. The same vibrations can be seen to have a substantial and deleterious effect on the spectroscopic signal produced by the conventional apparatus, despite its lesser degree of proximity to the source of

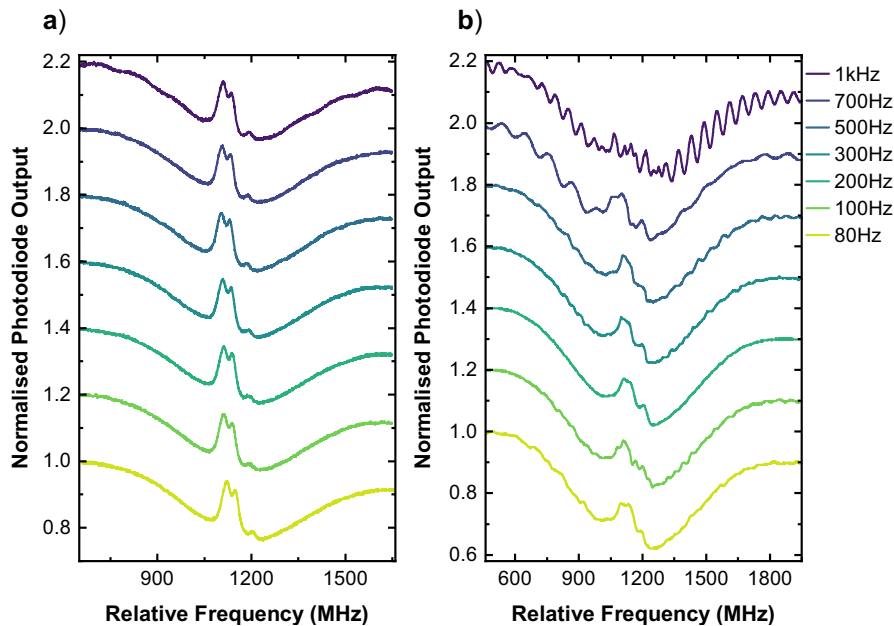


Fig. 8. The effect of different ranges of single-frequency vibrations on the saturated absorption spectroscopy signal of (a) the AM optical framework directly exposed to the vibrations, and (b) a conventional setup constructed on the other side of the same optical bench. For reference, the ^{85}Rb $F=3 \rightarrow F'=2,3$, and 4 transition is shown. As can be seen, the compact optical system exhibits a high level of resistance to vibrational disturbance, whereas the conventional setup is extremely susceptible to the same range of oscillations. For visibility, an offset of 0.2 is applied between successive traces.

the vibrations — see Fig. 8(b). The range of frequencies applied were between 80Hz and 1kHz with an amplitude of $\pm 0.2 \text{ ms}^{-2}$. Note that this measurement demonstrates that the compact system can be operated while the vibrations are applied without major disturbance. This clearly shows the advantages of compact AM-design, and additively manufactured frame, minimisation of the use of adjustable components and fully-surrounding support structures for the mechanical stabilisation of optical systems.

5. Conclusions and outlook

We have demonstrated a compact, inexpensive experimental system, based on 3D-printing methods, for performing Doppler-free spectroscopy on two lasers simultaneously, as well as generating an optical beat note with a third laser. Its response to vibrations and temperature changes has been analysed. We have thus demonstrated that the use of 3D-printing methods can lead to robust systems which can be tailored in performance to a required task. The demonstrated device shows comparable robustness against temperature changes and vibrations to specialised, integrated systems, but at a much lower cost. It is able to operate consistently over a 28 degree temperature range and in the presence of such vibrations as might be found in an un-isolated environment, demonstrating its suitability for use in portable quantum technologies. These methods are transferable and through the application of similar techniques to other complex optical systems are likely to transform current experimental hardware.

The system as shown is suitable for laser stabilisation for magneto-optical trapping, as needed for cold-atom-based quantum technologies. The use of the AM mount in this context allows an advanced design, tailored to the task, and can deliver high stability and reduced size and weight - and is thus relevant for the development of portable quantum technologies or the use of quantum technologies in space. In the future, the capacities of 3D printing can be exploited further by tailoring stiffness and thermo-mechanical response following optimisation in a computer simulation model e.g. via latticing, structural reinforcement or material combinations. We believe that our approach of using AM materials is critical for quantum technologies and applicable to all applications requiring fixed optical configurations.

Funding. School of Physics and Astronomy, University of Nottingham; European Commission (grant ErBeStA 800942); Engineering and Physical Sciences Research Council (EP/M013294/1, EP/R024111/1, EP/T001046/1).

Acknowledgment. We would like to thank Sarah Everton and Dominic Sims for useful comments, and Lisa Knbelreiter for assistance with data collection.

Disclosures. The authors declare the following competing interests: N.C., L.C. and L.H. are inventors on a UK pending patent application GB 1916446.6 (applicant: University of Nottingham, inventors: Nathan Cooper, Lucia Hackermüller, Laurence Coles) for the device described in the article.

Data Availability. All data necessary to support the conclusions of the article are presented in the article. Any additional data related to this paper may be obtained from the authors upon reasonable request.

References

1. F. Yver, A. Landragin, N. Dimarcq, A. Clairon, D. Holleville, P. Cheinet, P. Bouyer, C. Salomon, and C. Borde, "A cold atom interferometer for high precision measurements," in *2003 European Quantum Electronics Conference. EQEC 2003 (IEEE Cat No. 03TH8665)*, (IEEE, 2003), p. 309.
2. R. Geiger, A. Landragin, S. Merlet, and F. Pereira Dos Santos, "High-accuracy inertial measurements with cold-atom sensors," *AVS Quantum Sci.* **2**(2), 024702 (2020).
3. G. M. Tino, "Testing gravity with cold atom interferometry: Results and prospects," *Quantum Sci. Technol.* **6**(2), 024014 (2021).
4. L. Cacciapuoti, M. Armano, R. Much, O. Sy, A. Helm, M. P. Hess, J. Kehrer, S. Koller, T. Niedermaier, F. X. Esnault, D. Massonnet, D. Goujon, J. Pittet, P. Rochat, S. Liu, W. Schaefer, T. Schwall, I. Prochazka, A. Schlicht, U. Schreiber, P. Delva, C. Guerlin, P. Laurent, C. L. Poncin-Lafitte, M. Lilley, E. Savalle, P. Wolf, F. Meynadier, and C. Salomon, "Testing gravity with cold-atom clocks in space," *Eur. Phys. J. D* **74**(8), 164 (2020).
5. M. Takamoto, I. Ushijima, N. Ohmae, T. Yahagi, K. Kokado, H. Shinkai, and H. Katori, "Test of general relativity by a pair of transportable optical lattice clocks," *Nat. Photonics* **14**(7), 411–415 (2020).

6. F. Kaiser, P. Vergyris, A. Martin, D. Aktas, M. P. D. Micheli, O. Alibart, and S. Tanzilli, "Quantum optical frequency up-conversion for polarisation entangled qubits: towards interconnected quantum information devices," *Opt. Express* **27**(18), 25603–25610 (2019).
7. J. P. Hogue, S. Downes, C. MacCormick, and P. E. Kornilovitch, "Cold rydberg atoms for quantum simulation of exotic condensed matter interactions," *J. Supercond. Nov. Magn.* **27**(4), 937–940 (2014).
8. M. Lewenstein, A. Sanpera, V. Ahufinger, B. Damski, A. Sen, and U. Sen, "Ultracold atomic gases in optical lattices: mimicking condensed matter physics and beyond," *Adv. Phys.* **56**(2), 243–379 (2007).
9. E. Demler and T. Kitagawa, "Strongly correlated systems in atomic and condensed matter physics," *Lect. Notes Phys.* **284**, 28 (2014).
10. F. Dalfovo, S. Giorgini, L. P. Pitaevskii, and S. Stringari, "Theory of bose-einstein condensation in trapped gases," *Rev. Mod. Phys.* **71**(3), 463–512 (1999).
11. A. J. Leggett, "Bose-einstein condensation in the alkali gases: Some fundamental concepts," *Rev. Mod. Phys.* **73**(2), 307–356 (2001).
12. I. Bloch, J. Dalibard, and W. Zwerger, "Many-body physics with ultracold gases," *Rev. Mod. Phys.* **80**(3), 885–964 (2008).
13. S. Giorgini, L. P. Pitaevskii, and S. Stringari, "Theory of ultracold atomic fermi gases," *Rev. Mod. Phys.* **80**(4), 1215–1274 (2008).
14. P. Farrera, G. Heinze, B. Albrecht, M. Ho, M. Chávez, C. Teo, N. Sangouard, and H. De Riedmatten, "Generation of single photons with highly tunable wave shape from a cold atomic ensemble," *Nat. Commun.* **7**(1), 13556 (2016).
15. J. J. Garcia-Ripoll, P. Zoller, and J. I. Cirac, "Quantum information processing with cold atoms and trapped ions," *J. Phys. B At. Mol. Opt. Phys.* **38**(9), S567–S578 (2005).
16. I. I. Ryabtsev, I. I. Beterov, D. B. Tretyakov, V. M. Entin, and E. A. Yakshina, "Spectroscopy of cold rubidium rydberg atoms for applications in quantum information," *Phys.-Uspekhi* **59**(2), 196–208 (2016).
17. P. Roztocky, M. Kues, C. Reimer, B. Wetzell, S. Sciara, Y. Zhang, A. Cino, B. E. Little, S. T. Chu, D. J. Moss, and R. Morandotti, "Practical system for the generation of pulsed quantum frequency combs," *Opt. Express* **25**(16), 18940–18949 (2017).
18. P. Schneeweiss, A. Dureau, and C. Sayrin, "Cold-atom-based implementation of the quantum rabi model," *Phys. Rev. A* **98**(2), 021801 (2018).
19. A. Kuzmich, W. Bowen, A. Boozer, A. Boca, C. Chou, L.-M. Duan, and H. Kimble, "Generation of nonclassical photon pairs for scalable quantum communication with atomic ensembles," *Nature* **423**(6941), 731–734 (2003).
20. X.-H. Bao, A. Reingruber, P. Dietrich, J. Rui, A. Dück, T. Strassel, L. Li, N.-L. Liu, B. Zhao, and J.-W. Pan, "Efficient and long-lived quantum memory with cold atoms inside a ring cavity," *Nat. Phys.* **8**(7), 517–521 (2012).
21. K. Bongs, J. Malcolm, C. Ramello, L. Zhu, V. Boyer, T. Valenzuela, J. Maclean, A. Piccardo-Selg, C. Mellor, T. Fernholz, M. Fromhold, P. Krüger, O. Hellmig, A. Grote, S. Dörscher, H. Duncker, P. Windpassinger, K. Sengstock, C. Becker, B. Pelle, A. Hilico, M. Zhou, M.-C. Angonin, P. Wolf, F. P. Dos Santos, F. Bertoldi, P. Bouyer, T. Mazzoni, N. Poli, F. Sorrentino, M. Tarallo, G. Tino, S. Stellmer, F. Schreck, M. Popp, W. Herr, T. Wendrich, W. Ertmer, E. Rasel, and A. Kürbis, "A. Wicht, "iSense: A technology platform for cold atom based quantum technologies," in *Quantum Information and Measurement*, (Optical Society of America, 2014), pp. QTu3B–1.
22. S. Falke, N. Lemke, C. Grebing, B. Lipphardt, S. Weyers, V. Gerginov, N. Huntemann, C. Hagemann, A. Al-Masoudi, S. Häfner, S. Vogt, U. Sterr, and C. Lisdat, "A strontium lattice clock with 3×10^{-17} inaccuracy and its frequency," *New J. Phys.* **16**(7), 073023 (2014).
23. A. D. Ludlow, M. M. Boyd, J. Ye, E. Peik, and P. O. Schmidt, "Optical atomic clocks," *Rev. Mod. Phys.* **87**(2), 637–701 (2015).
24. F. Riehle, "Optical clock networks," *Nat. Photonics* **11**(1), 25–31 (2017).
25. S. L. Kemp, K. L. Butler, R. Freytag, S. A. Hopkins, E. A. Hinds, M. R. Tarbutt, and S. L. Cornish, "Production and characterization of a dual species magneto-optical trap of cesium and ytterbium," *Rev. Sci. Instrum.* **87**(2), 023105 (2016).
26. N. Cooper, L. Coles, S. Everton, I. Maskery, R. Champion, S. Madkhaly, C. Morley, J. O'Shea, W. Evans, R. Saint, P. Krüger, F. Orucevic, C. Tuck, R. Wildman, T. Fromhold, and L. Hackermüller, "Additively manufactured ultra-high vacuum chamber for portable quantum technologies," *Addit. Manuf.* **40**, 101898 (2021).
27. S. Madkhaly, L. Coles, C. Morley, C. Colquhoun, T. Fromhold, N. Cooper, and L. Hackermüller, "Performance-optimized components for quantum technologies via additive manufacturing," *PRX Quantum* **2**(3), 030326 (2021).
28. B. H. Jared, M. A. Aguilo, L. L. Beghini, B. L. Boyce, B. W. Clark, A. Cook, B. J. Kaehr, and J. Robbins, "Additive manufacturing: Toward holistic design," *Scr. Mater.* **135**, 141–147 (2017).
29. J. P. McGilligan, P. F. Griffin, R. Elvin, S. J. Ingleby, E. Riis, and A. S. Arnold, "Grating chips for quantum technologies," *Sci. Rep.* **7**(1), 384 (2017).
30. V. Schkolnik, K. Döringshoff, F. B. Gutsch, M. Oswald, T. Schuldt, C. Braxmaier, M. Lezius, R. Holzwarth, C. Kürbis, A. Bawamia, M. Krutzik, and A. Peters, "Jokarus-design of a compact optical iodine frequency reference for a sounding rocket mission," *EPJ Quantum Technol.* **4**(1), 9–10 (2017).
31. A. Strangfeld, S. Kanthak, M. Schiemangk, B. Wiegand, A. Wicht, A. Ling, and M. Krutzik, "Prototype of a compact rubidium-based optical frequency reference for operation on nanosatellites," *J. Opt. Soc. Am. B* **38**(6), 1885–1891 (2021).

32. A. Belenchia, M. Carlesso, Ö. Bayraktar, D. Dequal, I. Derkach, G. Gasbarri, W. Herr, Y. L. Li, M. Rademacher, J. Sidhu, D. K. Oi, S. T. Seidel, R. Kaltenbaek, C. Marquardt, H. Ulbricht, V. C. Usenko, L. Wörner, A. Xuereb, M. Paternostro, and A. Bassi, "Quantum physics in space," *Phys. Rep.* **951**, 1–70 (2022).
33. K. Frye, S. Abend, W. Bartosch, A. Bawamia, D. Becker, H. Blume, C. Braxmaier, S.-W. Chiow, M. A. Efremov, W. Ertmer, P. Fierlinger, T. Franz, N. Gaaloul, J. Grosse, C. Grzeschik, O. Hellmig, V. A. Henderson, W. Herr, U. Israelsson, J. Kohel, M. Krutzik, C. Kürbis, C. Lämmerzahl, M. List, D. Lüdtko, N. Lundblad, J. P. Marburger, M. Meister, M. Mihm, H. Müller, H. Müntinga, A. M. Nepal, T. Oberschulte, A. Papakonstantinou, J. Perovsek, A. Peters Achim, Prat E. M. Rasel, A. Roura, M. Sbroscia, W. P. Schleich, C. Schubert, S. T. Seidel, J. Sommer, C. Spindeldreier, D. Stamper-Kurn, B. K. Stuhl, M. Warner, T. Wendrich, A. Wenzlawski, A. Wicht, P. Windpassinger, N. Yu, and L. Wörner, "The bose-einstein condensate and cold atom laboratory," *EPJ Quantum Technol.* **8**(1), 1 (2021).
34. A. Bertoldi, K. Bongs, P. Bouyer, O. Buchmueller, B. Canuel, L.-I. Caramete, M. L. Chiofalo, J. Coleman, A. De Roeck, J. Ellis, P. W. Graham, M. G. Haehnelt, A. Hees, J. Hogan, W. von Klitzing, M. Krutzik, M. Lewicki, C. McCabe, A. Peters, E. Rasel, A. Roura, D. Sabulsky, S. Schiller, C. Schubert, C. Signorini, F. Sorrentino, Y. Singh, G. M. Tino, V. Vaskonen, and M.-S. Zhan, "Aedge: Atomic experiment for dark matter and gravity exploration in space," *Exp. Astron.* **51**(3), 1417–1426 (2021).
35. E. R. Elliott, M. C. Krutzik, J. R. Williams, R. J. Thompson, and D. C. Aveline, "Nasa's cold atom lab (cal): system development and ground test status," *NPJ Microgravity* **4**(1), 16 (2018).
36. N. Cooper, S. Madkhaly, D. Johnson, D. Baldolini, and L. Hacker Müller, "Dual-frequency spectroscopy for compact systems and enhanced laser stabilisation," arXiv preprint arXiv:2106.11014 (2021).
37. Ultimaker, "The widest material choice on the market (2011-2020)," <https://ultimaker.com/materials>.
38. Simplify3D, "Filament properties table," <https://www.simplify3d.com/support/materials-guide/properties-table/> (2021).
39. K. Friedrich and R. Walter, *Structure and Properties of Additive Manufactured Polymer Components* (Woodhead Publishing, 2020).
40. D. W. Preston, "Doppler-free saturated absorption: Laser spectroscopy," *Am. J. Phys.* **64**(11), 1432–1436 (1996).
41. G. D. Goh, Y. L. Yap, H. Tan, S. L. Sing, G. L. Goh, and W. Y. Yeong, "Process–structure–properties in polymer additive manufacturing via material extrusion: A review," *Crit. Rev. Solid State Mater. Sci.* **45**(2), 113–133 (2020).
42. H. Duncker, O. Hellmig, A. Wenzlawski, A. Grote, A. J. Rafipoor, M. Rafipoor, K. Sengstock, and P. Windpassinger, "Ultrastable, zerodur-based optical benches for quantum gas experiments," *Appl. Opt.* **53**(20), 4468–4474 (2014).
43. S. Ressel, M. Gohlke, D. Rauen, T. Schuldt, W. Kronast, U. Mescheder, U. Johann, D. Weise, and C. Braxmaier, "Ultrastable assembly and integration technology for ground-and space-based optical systems," *Appl. Opt.* **49**(22), 4296–4303 (2010).
44. V. Chonhenchob, S. P. Singh, J. J. Singh, J. Stallings, and G. Grewal, "Measurement and analysis of vehicle vibration for delivering packages in small-sized and medium-sized trucks and automobiles," *Packaging Technol. Sci.* **25**(1), 31–38 (2012).
45. V. Schkolnik, O. Hellmig, A. Wenzlawski, J. Grosse, A. Kohfeldt, K. Döringshoff, A. Wicht, P. Windpassinger, K. Sengstock, C. Braxmaier, M. Krutzik, and A. Peters, "A compact and robust diode laser system for atom interferometry on a sounding rocket," *Appl. Phys. B* **122**(8), 217 (2016).